2023 IEEE/ASME International Conference on Advanced Intelligent Mechatronics (AIM)
June 28-30, 2023. Seattle, Washington, USA

Continuous Dynamic Wireless Power Transfer for Circular Roadway with Optimal Load: Design and Analysis

Chen-En Lee, Sheng-Feng Lin, and Yen-Chen Liu

***Abstract*—The importance of dynamic wireless power transfer (DWPT) has increased significantly resulting from the development of electric mobility devices (EMDs). How to enlarge endurance with limited battery capacity has become a vital issue in the studies of EMDS, and the DWPT system has been foreseen as an emerging technology for this issue. In this paper, a continuous DWPT system has been investigated with the use of DD-shaped (bipolar) coils and Q-shaped (unipolar) coils in order to solve the problem of output power pulsation during the movement. To meet the practice of curved roadways and transfer efficiency, the design and analysis of transmitters and receivers for circular and athletic-field-like roadways are presented. The coupling coefficients and mutual inductance of the continuous DWPT system are addressed provided simulation validation and experimental test.**

***Keywords*—Dynamic wireless power transfer (DWPT), optimal load, circular roadway, stable output power.**

I. Introduction

Due to the industrial revolution, energy issues have always been an important topic. Till now, electricity has gradually become an alternative energy source for fossil fuels. Especially in recent years, the awareness of carbon reduction has risen. Electric vehicles (EVs) have become increasingly important. Similarly, due to the growing amounts of unmanned factories, there are a large number of automated guided vehicles (AGV) [1] and autonomous mobile robots (AMR) needed. Therefore, the way to charge these electric mobility devices (EMDs) is a vital topic. It's better to charge these devices wirelessly to prevent wire entanglement caused by conventional plug-in charging. Wireless power transfer (WPT) can transfer power without wire. In order to decrease the volume of the battery and charging time, dynamic wireless power transfer (DWPT) is applied to charge the EMDs. By using the DWPT system, the EMDs can be continuously powered by the transmitter coils laid under the roadway while in motion.

The transmitter coils under the roadway are coupling the receiver coil installed on the EMDs. The source side for the transmitter coils is the primary side, and the receiver coil for the charging devices is the secondary side. The coupling occurs between the primary side and the secondary side from the transmitters to the receiver. The coupling relation depends on the mutual inductance and the self-inductance of the transmitter coils and receiver coils. Hence, the coil structure, coil shape, and the air gap between the primary side and the secondary side that change the inductance will affect the coupling coefficient. For the coil structure, there are two main kinds of coils: long-track-loop type [2] and multiple-individual type. To reduce parasitic resistance on the long-track-loop type transmitters and endure continuous power transfer, this paper focuses on the design of multiple-individual transmitters.

The power null phenomenon happens when the receiver is on the gap between transmitters where low power transfers. Furthermore, there are still power pulsation issues that need to solve because of the movement of the receiver. The power pulsation may damage the charging device or make the output unstable. Thus, it's important to get a stable output to protect the charging devices.

There are two methods to deal with power pulsation, compensation topology [3] and coil shape [4]. The research [5] of compensation circuits proposed LCL or LCC topology because of its independence of the load. Once there is horizontal misalignment while moving between the transmitters and the receiver, the current will drain from the source and won't damage the DWPT system in LCC topology [6]. Consequently, an LCC-S compensation topology is applied in this paper [7].

Regarding the method for adjusting coil shapes, the authors in [8] proposed a new structure coil DD-shaped (bipolar) and Q-shaped (unipolar) coils that decoupled naturally to cope with the power null phenomenon and power pulsation. However, the proposed track of DD-shaped coils and Q-shaped coils is linear. The results only show the behavior of the finite track and are measured statically. The linear roadway will limit the track so that the receiver speed can't be considered dynamically. Hence, the researcher in [9] proposed a circular roadway formed from twenty DD-shaped coils and Q-shaped coils. Nevertheless, the actual road is not a straight long linear track or a fixed radius circular roadway.

This study intends to synthesize the results of the different track designs and discuss the shape design of different DD-coils and Q-coils. The actual road can be disassembled into several sections with different shapes of track designs. Similarly, the DD-Q coil structure is adopted as the receiver and the optimal size is discussed. This paper finds out an optimal receiver coil size that is different from the transmitter coil size by finite element analysis (FEA) software ANSYS Maxwell. With the optimal receiver coil size, the pulsation of mutual inductance between the receiver and transmitters can be reduced. The optimal load of this DWPT system is found and applied to get the maximum efficiency of the system.

This work was supported by the National Science and Technology Council (NSTC), Taiwan, under Grant NSTC 112-2636-E-006-001.

C.-E. Lee, S.-F. Lin, and Y.-C. Liu are with the Department of Mechanical Engineering, National Cheng Kung University, Tainan 70101, Taiwan. E-mail: {n16101727@ncku.edu.tw, stuman861026@gmail.com, yliu@mail.ncku.edu.tw}.

Consequently, this study focuses on analyzing the combination of the different track-coil designs and optimizing the size of the receiver which considers the segmented control [10].

The rest of this paper is organized as follows. Preliminary and system configurations are presented in Section II. In Section III, the design and analyses of transmitter and receiver coils are presented with simulation results. Experimental results of a circular roadway with an optimal load are illustrated in Section IV. Finally, the conclusion and future work are stated in Section V.

II. System Configuration and Circuit Modeling

The system configuration, as shown in Fig. 1, and the behavior of the LCC-S compensation circuit based on Faraday's Law are addressed in this section. Additionally, the circuit analysis of the continuous DWPT system is illustrated as the preliminary.

A. Preliminary and System Configuration

Based on Faraday's Law, the magnetic flux variation is necessary between the transmitters and the receiver so that the power can be transmitted wirelessly. Hence, the power in the transmitters and the receiver should be alternating. A converter is needed to transfer the source from direct current (DC) to alternating current (AC). Therefore, the system configuration considered in the DWPT is shown in Fig. 1 utilizing an LCC-S topology [7]. The DC source, V_{inDC} input voltage is transferred to AC input voltage V_{inAC} by a full-bridge inverter, which is composed of four MOSFETs M_1-M_4. As the output on the receiver is also alternating, the output voltage V_{outAC} needs a full-bridge rectifier to transfer AC power to DC power. The rectifier is constructed from four diodes D_1-D_4. C_f is the filter capacitor, and R_{load} is the load of the system.

In the continuous DWPT system, only a few of the transmitters in the vicinity of the receiver would generate magnetic flux. The remaining transmitters far from the location of the receiver only transfer negligible or zero power due to the low coupling. If all the transmitters are turned on, the uncoupled transmitters may cause power loss and electromagnetic interference (EMI). Hence, to ensure higher efficiency during the DWPT system, a segmented control, turning-off low coupling transmitters [11], is significant to enhance system performance. Furthermore, EMI can be prevented with segmented control for safety issues in the DWPT system. To cope with this issue, the segmented activation control is proposed by turning the switches of the transmitters, S_1-S_{20} as shown in Fig. 1, on and off depending on the position of the receiver. The performance of the continuous DWPT system with respect to the number of activated transmitters is discussed in the next section.

Most of the previous research in the development of DWPT focuses on a long-linear track [1], [8]; however, such designs and analyses cannot be directly applied on curved roadways which are very common in practice. Therefore, in this paper, the various designs of curved roadways, including circular and athletic-field-like roadways, as seen in Fig. 2 and Fig. 3, with annulus sector and rectangular receivers, are investigated. These designs are implemented based on the LCC-S compensation topology circuit [5] as shown in Fig. 1. It is noted that the radius and geometry of the primary side in Fig. 2 and Fig. 3 are only an illustration, and a variety of designs can be adopted based on the following studies.

B. Circuit Analysis and Optimal Load

The fundamental harmonic analysis can be applied because of the high-quality factors in the DWPT system [12]. Hence, the relationship between the input voltage of the inverter V_{inDC} and the output voltage of the inverter V_{inAC} can be derived as

$$V_{inAC} = \frac{4}{\sqrt{2}\pi} V_{inDC}. \tag{1}$$

The wireless system transmits power by the resonant conditions that can be adjusted by electronic components in the LCC-S compensation circuit as shown in Fig.1. The designs of DD-shaped coils and Q-shaped coils are arranged in a linear way and are proven decoupled in [8] to each transmitter coil. According to this, each compensation circuit loop can be designed independently.

The combination of the first inductance L_{tpi} on the transmitter side and the first capacitance C_{tpi} on the transmitter side as the primary inductor L'_{tpi} can be expressed as

$$L'_{tpi} = L_{tpi} - \frac{1}{\omega^2 C_{tpi}} \ (i = 1, ..., N), \tag{2}$$

where ω is the angular frequency of the inverter with $\omega = 2\pi f$, f is switching frequency, and N is the number of transmitters in the primary side of the DWPT system. Generally, the switching frequency can be chosen as 85kHz according to the standard of SAE J2954.

Thus, the resonance compensation parameters are derived from equations as follows

$$L_{tsi} = L'_{tpi} = \frac{1}{\omega^2 C_{tsi}}, \ L_r = \frac{1}{\omega^2 C_r}. \tag{3}$$

Hence, the current in the transmitter can be derived as

$$I_{tpi} = \frac{V_{inAC}}{j\omega L_{tsi}}. \tag{4}$$

The above equation demonstrates that the current in the transmitter I_{tpi} would be the same in each circuit once the L_{tsi} are chosen as the same value L_{ts}. By considering the same value of L_{tsi}, substituting (1) into (4) lead to the generalized I_{tpi} that can be rewritten as

$$I_{tp} = \frac{4}{\sqrt{2}\pi j\omega L_{ts}} V_{inDC}. \tag{5}$$

Note that, mutual inductance exists only when the transmitters are activated resulting from the segmented activation control. By denoting N_{act} the set of transmitters that are turned on for power transfer (in the vicinity of the receiver), the accumulated voltage V_{outAC} with identical L_{tsi} (3) can be expressed as

$$V_{outAC} = \sum_{i \in N_{act}} \{j\omega M_i I_{tpi}\} = j\omega M_{sum} I_{tp}, \tag{6}$$

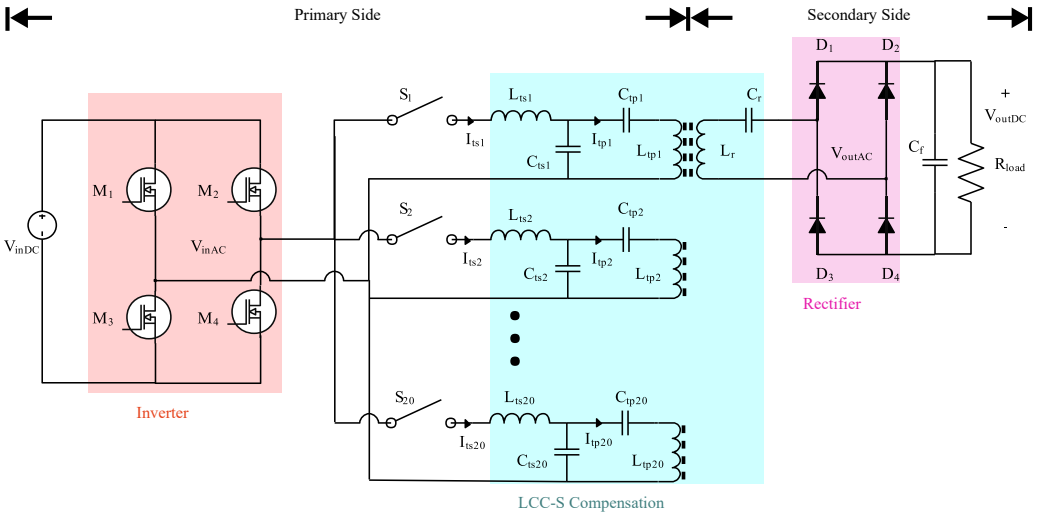

Fig. 1. Circuit of LCC-S compensation topology in the proposed continuous DWPT.

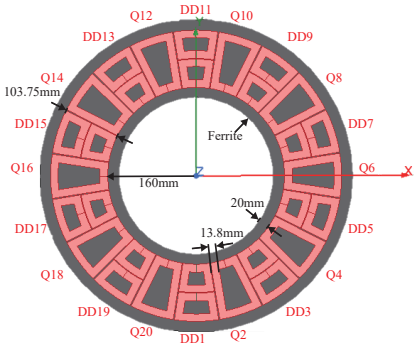

Fig. 2. Layout of transmitters in the primary side with a circular roadway.

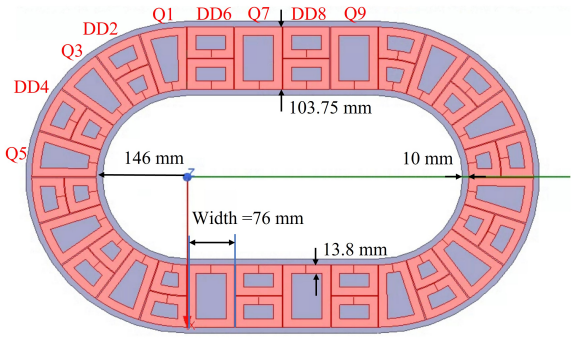

Fig. 3. Layout of transmitters in the primary side with an athletic-field-like roadway.

where $M_i, i \in N_{act}$ is the mutual inductance between the receiver and the activated transmitters, and M_{sum} is the summation of the mutual inductance between the receiver and the turned-on transmitters.

On the secondary side, the output voltage after the rectifier V_{outDC} is the same as the inverter. Thus, the input and output voltages of the rectifier can be expressed as

$$V_{outAC} = \frac{4}{\sqrt{2}\pi} V_{outDC}. \tag{7}$$

By substituting (4) and (7) into (6), the relationship between the voltage of the input source and transferred output voltage can be simplified given as

$$V_{outDC} = \frac{M_{sum}}{L_{ts}} V_{inDC}. \tag{8}$$

In the above derivation, once L_{ts} and V_{inDc} are fixed, the output voltage is proportional to M_{sum}. In order to transfer stable power provided less pulsation, we need to keep M_{sum} as stable as possible which means that the variation of M_{sum} should be as minimized as possible.

A maximum efficiency transfer capability is considered an important performance index of the DWPT systems. To get the optimal load for maximum efficiency, the parasitic resistance in each inductor should be considered, and the subscripts of the parasitic resistance come after the inductors. Note that, R_{ts}, R_{tp}, and R_r corresponds to the parasitic resistance of L_{ts}, L_{tp}, and L_r. For the rectifier circuit, the relationship between the input equivalent resistance R_{eq} and the output resistance R_{load} can be expressed as

$$R_{eq} = \frac{8}{\pi^2} R_{load}. \tag{9}$$

By assuming that the switches of the rectifier are lossless, and the parasitic resistances for each circuit loop are the same, the efficiency of the multi-transmitter can be shown as

$$\eta = \frac{\omega^4 M_{sum}^2 L_{ts}^2 R_{eq}}{[R_{ts} A + \omega^2 L_{ts}^2] A (R_{eq} + R_r)^2}, \tag{10}$$

where the constant A is given as

$$A = \frac{\omega^2 M_{sum}^2}{R_{eq} + R_r} + R_{tp}.$$

By taking the derivative of the DWPT efficiency (10) with respect to R_{eq}, the optimal load condition based on maximizing

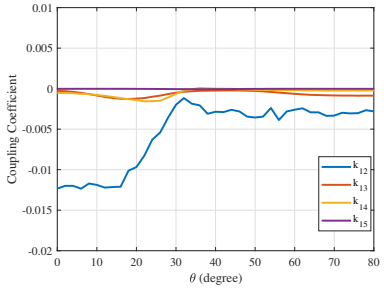

Fig. 4. Coupling coefficients between coils in circular roadways.

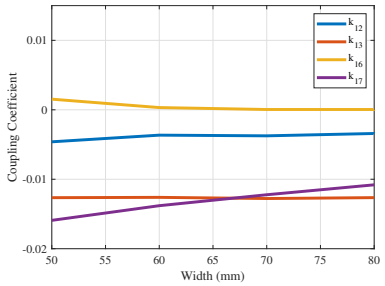

Fig. 5. Coupling coefficients between coils in athletic-field-like roadways.

the transferred efficiency can be obtained using

$$\frac{\partial \eta}{\partial R_{eq}} = 0.$$

Consequently, the optimal load resistance can be calculated as

$$R_{eq(opt)} = \sqrt{\frac{[\omega^2 M_{sum}^2 + R_{tp}R_r][R_{ts}\omega^2 M_{sum}^2 + \omega^2 L_{ts}^2 R_r + R_{tp}R_{ts}R_r]}{R_{tp}[R_{ts}R_{tp} + \omega^2 L_{ts}^2]}}. \tag{11}$$

With the impedance-matching method, the optimal load can be implemented by placing a power electronics converter such as a DC/DC converter on the secondary side to track the maximum efficiency [13]. Furthermore, with the converter introduced, the control method [14] can be applied to the DWPT system to track the desired output. The optimal load will be considered and implemented in the experimental validation in Section IV.

III. Magnetic Coupling Structure

A. Transmitter Coils on Primary Side

The design and order of DD-shaped coils and Q-shaped coils are mainly utilized to ensure inherent decoupling between the adjacent coils. Since the original design of the DD-Q combination was presented for linear tracks, in this section, we first conduct simulations to demonstrate that the DD-shaped and Q-shaped coils can ensure satisfactory performance in curved roadways. The results illustrated in this section were obtained by FEA software. In the simulations, k_{ij} is utilized to denote the coupling coefficients between the i-th coil to the j-th coil. If k_{ij} is small, then the coupling between these two coils is low. The coupling coefficient is defined from the mutual inductance and given as

$$k_{ij} = \frac{M_{ij}}{\sqrt{L_i L_j}}, \tag{12}$$

where M_{ij} is the mutual inductance between the i-th coil and the j-th coil, and L_i, L_j are the self-inductance of the i-th coil and the j-th coil.

The corresponding coupling coefficients with the roadways shown in Fig. 2 and Fig. 3 are illustrated in Fig. 4 and Fig. 5, respectively. In Fig. 4, the horizontal axis is the position of the receiver on the secondary side and the vertical axis is the coupling coefficient. As the result, each coupling coefficient is small enough to be neglected. The general coupling coefficient ranges from 5% to 30% (0.05-0.3) in the DWPT system. This means that even though the roadway is transferred to circular, the adjacent transmitter coils are naturally decoupled.

We consider the combination of the simple rectangle coils which are DD-shaped to be the same as Q-shaped and proposed circular coils in the same roadway. Place the rectangle coils and the proposed circular-type coils together as in Fig.3. The coupling coefficient is also simulated from FEA software shown in Fig.5. In Fig.5, the horizontal axis is the width of the rectangle coils where the Q-shaped rectangle coil is the same size as the DD-shaped rectangle coil, and the vertical axis is the coupling coefficient. As shown in the results, independent of the shape of the coils on the primary side, DD-shaped coils are always decoupled with Q-shaped coils. All in all, for both athletic-field-like roadways and circular roadways, DD-shaped and Q-shaped transmitter coils are naturally decoupled.

B. Receiver Coils on Secondary Side

The DD-shaped and Q-shaped coils are overlapped and connected in series as the receiver. To get a stable M_{sum}, the better way to design the receiver is similar to the shape of transmitters on the primary side as the circular sector shape shown in Fig.7. The angle of each coil is optimized as DD for $38.5°$and Q for 41.5 °by FEA software. The results of the mutual inductance based on the optimal design of the receiver are shown in Fig.6. Although the optimal design of the receiver makes the pulsation of M_{sum} less than 1%, the general coils are set as the rectangle coils. Therefore, we consider the simple rectangle coils of both DD-shaped and Q-shaped receivers of the general cases in this section.

Next, we analyze how the size of DD-Q coils on the receiver influences the M_{sum} based on the circular roadway transmitters as Fig.2. The design is under the assumption that DD-shaped coils have the same size as the Q-shaped coils and L_1 and L_2 are defined as shown in Fig. 9. In that, L_1 affects the coverage of the transmitters and L_2 decides the width of the receiver, as known as the width of the EMDs. If L_2 is larger, the tolerance of the misalignment can be more flexible. Fig. 10 shows the variation of L_2, the horizontal axis represents the position of the receiver and the vertical axis is the mutual

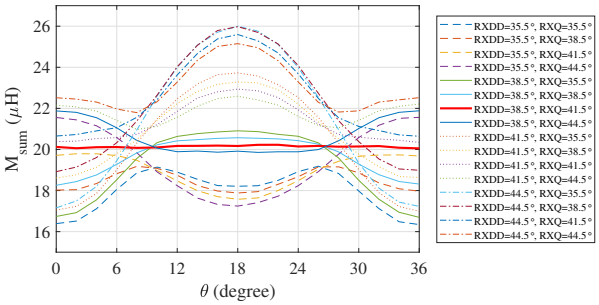

Fig. 6. Optimal design of annulus sector receivers for circular roadways.

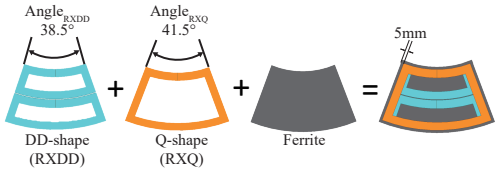

Fig. 7. Optimal design of annulus sector receivers for circular roadways.

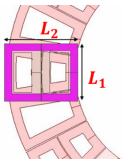

Fig. 9. Generalized design of rectangular receivers for athletic-field-like roadways.

inductance between the transmitters and the receiver. As the result, the pulsation will decrease when L_2 is larger than the transmitter. Although the high mutual inductance and less pulsation when L_2 is larger, we design L_2 as wide as the transmitter for the cost consideration. Because the pulsation is quite close when L_2 is wider than the transmitter, the mutual inductance does not increase a lot also. Hence, we simplify L_2 as $103.75mm$ with 1% pulsation will be easier.

Fig. 8 shows the mutual inductance with respect to various lengths L_1 when the receiver is moving as represented by θ. It is noted that when the receiver covers only one transmitter as known as $L_1 = 87mm$, the mutual inductance M_{sum} is more stable with less pulsation. As the mutual inductance raises with the increase of the coverage area, the pulsation rises up to about 8% when the coverage becomes larger. Until L_1 is larger than $143mm$ which covers two or more transmitters, the pulsation starts to decrease from 6%. In brief, optimizing the receivers needs to consider the shape of the transmitters and the coverage area of the transmitters. The wider the receivers overlap the transmitters, the higher the mutual inductance will be. According to (8), choose the required voltage gain based on the transmitters and the receiver design. Then, adjust the receiver size to reduce the pulsation of M_{sum}. Note that, totally covering the full DD-shaped coils or Q-shaped coils whose pulsation will be lower than covering only half DD-shaped coils or Q-shaped coils.

C. Segmented Activation Control for Transmitter Coils

Although the more transmitters are turned on, the more M_{sum} can be received on the secondary side, turning to many transmitters would reduce the system efficiency due to power loss. Hence, controlling the activation of transmitters according to the position of the receiver is essential. Fig. 11 shows the coupling coefficient between the transmitters and the receiver. Choose to turn on the higher coupling coefficient transmitters that are coupled with the receiver. As the result, only three or five transmitters in the neighborhood of the receiver the coupling coefficient are activated. For example, when the receiver is above the DD3 coil where θ is 36°, the Q2, DD3, and Q4 are coupling notable, and DD1 and DD5 are coupling with less coupling coefficient, those are enabled to transfer power. In addition to this, the case of

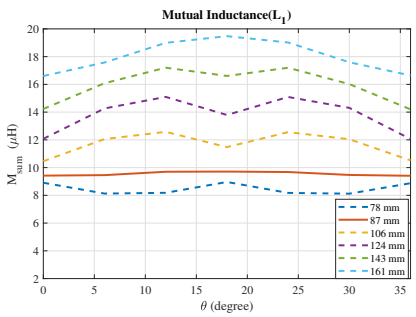

Fig. 8. Mutual inductance with regard of θ ranges for L_1.

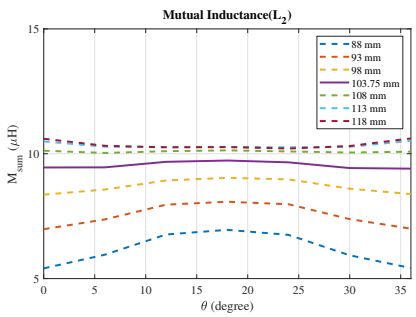

Fig. 10. Mutual inductance with regard of θ ranges for L_2.

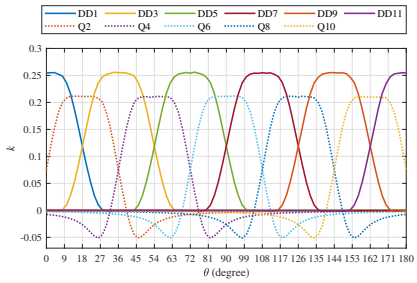

Fig. 11. Coupling coefficient between transmitters and receiver.

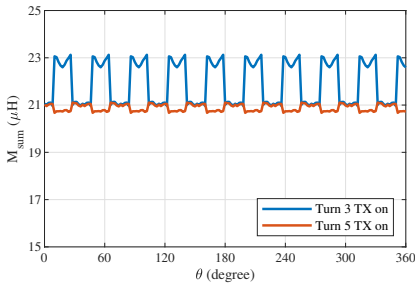

Fig. 12. Mutual inductance with a different number of enabled transmitters.

three activated transmitters has a higher M_{sum} than the case of five activated transmitters shown in Fig.12. Fig.12 shows the mutual inductance with turned-three-on and turned-five-on cases by the FEA software. Otherwise, the case of five activated transmitters has more stable M_{sum} than the case of three activated transmitters.

IV. Experimental Results

The experimental setup is shown in Fig.13, where the power is transferred from the primary side to the secondary side so as to drive a motor mounted in the center of the circular roadway [9]. The experiment is a prototype whose transmitters and the receiver are circular. The coil structure is realized on a nylon and acrylic base to prevent EMI issues. Transmitter coils and receiver coils are winding by Litz wire to prevent the skin effect. Each DD-shaped coil is winded in 10 turns at both parts and each Q-shaped coil is winded in 8 turns. The receiver moves along the roadway design as Fig.2 with a $20mm$ air gap. The ferrite plate with $2mm$ thickness is placed to prevent leakage flux. Power relays JY5H-K are chosen as the switches for segmented activation control. With the FEA software results about the coupling, we choose to turn on three transmitters to have stable and higher output. Both switching signals of the inverter and the rectifier are enhanced width modulation (ePWM) from the controller, TMS320F28335 chip (Texas Instrument). The duty cycle of both is 48%, and there is a phase difference π insuring zero voltage switching (ZVS) [15]. Achieve ZVS can decrease the loss of the switching and higher efficiency.

The receiver is set up as Fig.7, which is actuated by the center motor. The position information can be obtained from

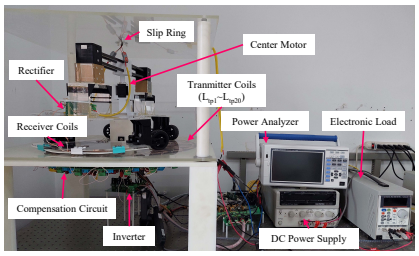

Fig. 13. Experimental setup with a circular roadway.

Symbol	Description of the parameter	Design Value
L_{tpi}	Transmitter Primary Inductance	$26.6\mu H$ (DD-shape) $15.4\mu H$ (Q-shape)
C_{tpi}	Transmitter Primary Capacitance	$0.2971\mu F$ (DD-shape) $5.842\mu F$ (Q-shape)
L_{tsi}	Transmitter Secondary Inductance	$14.8\mu H$
C_{tsi}	Transmitter Secondary Capacitance	$0.2369\mu F$
L_r	Receiver Inductance	$90.36\mu H$
C_r	Receiver Capacitance	$0.0388 + 0.0047\mu F$
C_f	Filter Capacitance	$1000 + 0.1\mu F$
V_{inDC}	DC input voltage	$12V$
R_{load}	The DC load of the system	20Ω

TABLE I
Parameters

the rotational speed ω_{rpm}. With the initial position θ_0, the position θ will be known as

$$\theta = \int \omega_{rpm} dt + \theta_0. \tag{13}$$

The load of the system is the center motor which is connected to the rectifier but finds the optimal load resistance first compared with the derivation as SectionII-B. The parameter in the coupling structure follows the results in SectionIII, which is listed in TableI. Note that the larger series capacitance C_f on the secondary side helps reach ZVS, and also filters low-frequency noise. On the other hand, smaller capacitance filters high-frequency noise.

To find out the optimal load, Fig.14 shows the efficiency with various loads. The simulated results $R_{load(opt)}$ is 24.14 Ω, and the experiment shows the peak of the efficiency is about 15Ω to 20Ω. Therefore, the optimal load is chosen as 20Ω, and the efficiency of the optimal load is about 72%. In order to apply the real situation, Dynamixel MX-106 is used as a central motor. To prevent the voltage pulsation that interrupts or damages the motor, the linear regulator L7812CV is added in front of the motor.

The input power for the DWPT system is 28.2 W for the application on the center motor and the output power is measured as 14.2 W. Fig.15 shows the efficiency with regard to the position of the receiver θ using a center motor as load and driving at 45 rpm as angular velocity. The efficiency is 50% which is less than the efficiency of the optimal load. With the optimal design of the transmitters, we get stable mutual inductance but need to consider the load situation. Furthermore, the motor can be seen as a varying load. The impedance of the motor changes depending on the operating situation. This means mismatching of the load may cause lower efficiency. In (11), the optimal load is found as a fixed point once the circuit is decided. Hence, to track the optimal

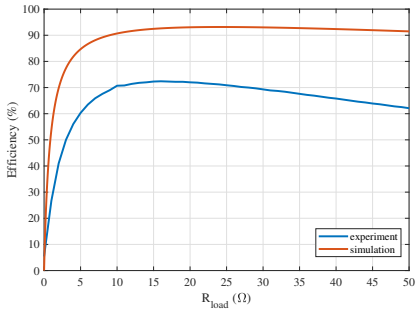

Fig. 14. Results of optimal load.

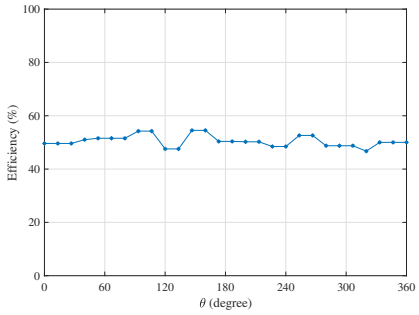

Fig. 15. Efficiency using a center motor as a load.

Literature	Power Level	Efficiency	Pulsation
[8]	384 W	90.37%	2%
[11]	183.3 W	84.9%	23.0%
This Work	28.2 W	72%	less than 1%

TABLE II
COMPARISONS BETWEEN OTHER WORKS

load in the DWPT system, the DC/DC converter is needed on the secondary side for the varying load.

The comparisons between previous studies and this work are listed in TableII. It can be found that the system efficiency is lower than any other work because this study is a low-power application on a motor. However, the output power pulsation is a particular concern in this work, whose pulsation is lower than others. If the transfer power increase, the transfer efficiency will enlarge.

V. Conclusion and Future Work

This paper analyzes the combinations of Q-shaped coils and DD-shaped coils in the DWPT system. On the primary side, DD-shaped coils are always naturally decoupling with Q-shaped coils for circular roadways and athletic-field-like roadways. For the receiver, the more coverage of the transmitters, the higher the mutual inductance will be. The experiment is set up as circular roadway transmitters and the optimized annulus-sector-shaped receiver. The segmented activation control is used and chooses to turn on three transmitters. The optimal load is found, and the efficiency is 72%. The center motor is applied, and the efficiency is 50% which is less than the optimal load. To track the optimal load based on the maximum efficiency for the varying load, the power converter is needed on the secondary side. In the future, a DC/DC converter can be applied to reach impedance-matching. Future work will also focus on independent control methods for both the primary side and the secondary side without information exchange.

References

[1] S.-J. Huang, T.-S. Lee, W.-H. Li, and R.-Y. Chen, "Modular on-road agv wireless charging systems via interoperable power adjustment," *IEEE Transactions on Industrial Electronics*, vol. 66, no. 8, pp. 5918–5928, 2018.

[2] J. Shin, S. Shin, Y. Kim, S. Ahn, S. Lee, G. Jung, S.-J. Jeon, and D.-H. Cho, "Design and implementation of shaped magnetic-resonance-based wireless power transfer system for roadway-powered moving electric vehicles," *IEEE Transactions on Industrial electronics*, vol. 61, no. 3, pp. 1179–1192, 2013.

[3] A. C. Bagchi, A. Kamineni, R. A. Zane, and R. Carlson, "Review and comparative analysis of topologies and control methods in dynamic wireless charging of electric vehicles," *IEEE Journal of Emerging and Selected Topics in Power Electronics*, vol. 9, no. 4, pp. 4947–4962, 2021.

[4] K. Kadem, M. Bensetti, Y. Le Bihan, E. Labouré, and M. Debbou, "Optimal coupler topology for dynamic wireless power transfer for electric vehicle," *Energies*, vol. 14, no. 13, p. 3983, 2021.

[5] U. D. Kavimandan, V. P. Galigekere, O. Onar, M. Mohammad, B. Ozpineci, and S. M. Mahajan, "The sensitivity analysis of coil misalignment for a 200-kw dynamic wireless power transfer system with an lcc-s and lcc-p compensation," in *2021 IEEE Transportation Electrification Conference & Expo (ITEC)*. IEEE, 2021, pp. 1–8.

[6] J.-S. Hu, F. Lu, C. Zhu, C.-Y. Cheng, S.-L. Chen, T.-J. Ren, and C. C. Mi, "Hybrid energy storage system of an electric scooter based on wireless power transfer," *IEEE Transactions on Industrial Informatics*, vol. 14, no. 9, pp. 4169–4178, 2018.

[7] Y. Chen, H. Zhang, S.-J. Park, and D.-H. Kim, "A switching hybrid lcc-s compensation topology for constant current/voltage ev wireless charging," *Ieee Access*, vol. 7, pp. 133 924–133 935, 2019.

[8] Y. Li, J. Hu, T. Lin, X. Li, F. Chen, Z. He, and R. Mai, "A new coil structure and its optimization design with constant output voltage and constant output current for electric vehicle dynamic wireless charging," *IEEE Transactions on Industrial Informatics*, vol. 15, no. 9, pp. 5244–5256, 2019.

[9] A. Y. Dwinanto and Y.-C. Liu, "Design and analysis for dynamic wireless power transfer based on circular railway with continuous dynamic loads," in *2021 IEEE/ASME International Conference on Advanced Intelligent Mechatronics (AIM)*. IEEE, 2021, pp. 1075–1082.

[10] X. Li, J. Hu, H. Wang, X. Dai, and Y. Sun, "A new coupling structure and position detection method for segmented control dynamic wireless power transfer systems," *IEEE Transactions on Power Electronics*, vol. 35, no. 7, pp. 6741–6745, 2020.

[11] Y. Luo, Y. Song, Z. Wang, R. Mai, B. Yang, and Z. He, "Auto-segment control system with high spatially average power for dynamic inductive power transfer," *IEEE Transactions on Transportation Electrification*, 2022.

[12] H. Li, J. Li, K. Wang, W. Chen, and X. Yang, "A maximum efficiency point tracking control scheme for wireless power transfer systems using magnetic resonant coupling," *IEEE Transactions on Power Electronics*, vol. 30, no. 7, pp. 3998–4008, 2014.

[13] X. Hu, Y. Wang, Y. Jiang, W. Lei, and X. Dong, "Maximum efficiency tracking for dynamic wireless power transfer system using lcc compensation topology," in *2018 IEEE Energy Conversion Congress and Exposition (ECCE)*. IEEE, 2018, pp. 1992–1996.

[14] Z. Zhou, L. Zhang, Z. Liu, Q. Chen, R. Long, and H. Su, "Model predictive control for the receiving-side dc–dc converter of dynamic wireless power transfer," *IEEE Transactions on Power Electronics*, vol. 35, no. 9, pp. 8985–8997, 2020.

[15] X. Wang, J. Xu, M. Leng, H. Ma, and S. He, "A hybrid control strategy of lcc-s compensated wpt system for wide output voltage and zvs range with minimized reactive current," *IEEE Transactions on Industrial Electronics*, vol. 68, no. 9, pp. 7908–7920, 2020.